

IGA REWERS, TERESA SERUGA, MAGDA KIJANIA\*

## $M_{Rd} - N_{Rd}$ INTERACTION CURVES WITH ANALYSIS OF SECOND ORDER EFFECTS FOR REINFORCED CONCRETE COLUMNS

### KRZYWE INTERAKCJI $M_{Rd} - N_{Rd}$ Z ANALIZĄ EFEKTÓW II RZĘDU DLA SŁUPÓW ŻELBETOWYCH

#### Abstract

The paper presents regulations for evaluating  $M_{Rd} - N_{Rd}$  interaction curves for reinforced concrete members subjected to axial force and bending moments in one plane, comparing two simplified methods. An example for application of interaction curves in designing columns was presented. The latter part of the paper consists of two simplified methods of designating second order effects according to EC2 – nominal curvature method, nominal stiffness method. The comparison of them was made with  $M_{Rd} - N_{Rd}$  interaction curves.

*Keywords: reinforced concrete column, interaction curve, second order, nominal stiffness, nominal curvature*

#### Streszczenie

W artykule przedstawiono zasady wykonywania krzywych interakcji  $M_{Rd} - N_{Rd}$  dla przekrojów elementów żelbetowych, obciążonych siłą osiową i momentem zginającym w jednej płaszczyźnie, porównując dwie metody uproszczone ich opracowywania. Zaprezentowano również przykład zastosowania krzywych interakcji do doboru zbrojenia słupów krępych. W dalszej części pracy zawarto porównanie dwóch uproszczonych metod wyznaczania efektów II rzędu wg EC2 – metody nominalnej krzywizny i metody nominalnej sztywności, wykonane przy pomocy krzywych interakcji  $M_{Rd} - N_{Rd}$ .

*Słowa kluczowe: słupy żelbetowe, krzywa interakcji, efekty II rzędu, nominalna sztywność, nominalna krzywizna*

\* M.Sc. Eng. Iga Rewers, Ph.D. Eng. Teresa Seruga, M.Sc. Eng. Magda Kijania, Institute of Building Materials and Structures, Faculty of Civil Engineering, Cracow University of Technology.

## 1. Introduction

### 1.1. The purpose and scope of the article

The following paper presents regulations of determining  $M_{Rd} - N_{Rd}$  interaction curves, comparing two different methods [5, 16] (including an easy method suitable for creating spreadsheets). In the latter part of the article, two simplified methods of evaluating second order effects according to EC2 [17] were compared – nominal stiffness method (MNS) and nominal curvature method (MNC).

The article is not intended to assess the accuracy of methods of MNS and MNC, because such an assessment can be credible only on the basis of experimental results. The aim of the paper is to indicate the need for comments to EC2 [17], which could be followed when choosing the method of calculating the second order effects.

The following comparison was made by placing values of second order moments on the interaction curves. In the analysis column, the slenderness  $\lambda, \lambda/\lambda_{lim}$  ratio, the reinforcement ratio and an effective creep coefficient were variable.

The article also presents an example of using interaction curves in designing reinforced concrete columns.

### 1.2. Interaction curves

The load-bearing capacity of a cross-section subjected to an axial force and a bending moment in one plane can be illustrated by an  $M_{Rd} - N_{Rd}$  interaction curve. An area created by the curve presents permissible values of pairs of generalised forces. A point ( $M_{Ed}, N_{Ed}$ ) beyond the interaction curve means an exceeding of the ultimate limit state.

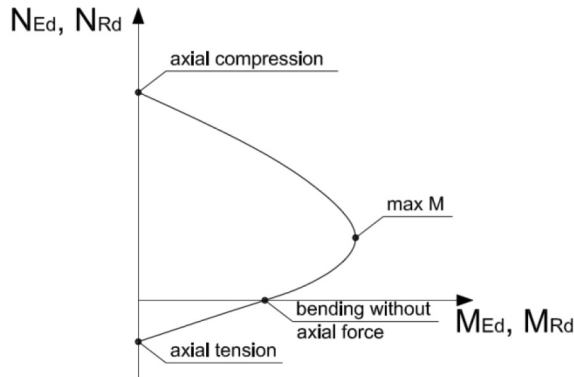


Fig. 1.  $M_{Rd} - N_{Rd}$  interaction curve with designated cases of concrete cross-section work

Interaction curves for assumed steel and concrete grades, reinforcement ratios and dimensions ratios, presented as nomograms suitable for designers are published in books and resources for designers. A set of such nomograms for different shapes of cross-sections is included for example in [1], and in CEB/FIP Manual on Bending and Compression Design

of Sections under Axial Action Effects at the Ultimate Limit State [2]. In paper [3] there is a graph presenting a possible simplification of the  $M_{Rd} - N_{Rd}$  interaction curve (Fig. 2).

Basic information and examples of nomograms were also included in M. Knauff's recently published book [4]. A detailed description of this issue can be found in R. Kliszczewicz paper [5].

$M_{Rd} - N_{Rd}$  interaction curves used and presented in papers and in specialist software [6, 7, 8, 9, 10, 11, 12, 13] are not commonly used in engineering projects. Not much attention is paid to this issue also in students books and teaching resources. However, interaction curves and nomograms based on them are popular in other countries [14, 15], for instance, they are found in a large part of an academic book for designing concrete structures, published by ČVUT in Prague [16].

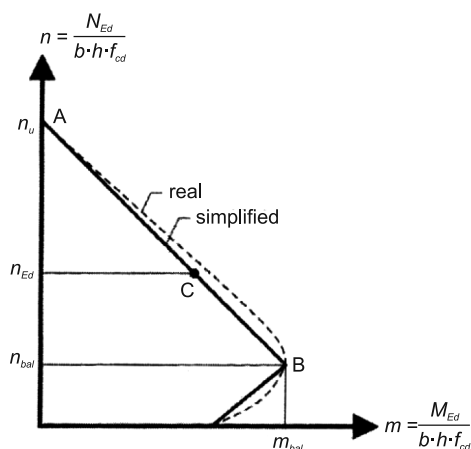


Fig. 2. Possible simplification of an  $M_{Rd} - N_{Rd}$  interaction curve (according to [3])

## 2. Creating interaction curves with simplified methods

Drawing an interaction curve for reinforced concrete cross-sections is possible not only with a general method, but also with a so-called partly-simplified method [5]. This one is significantly easier in calculations, whilst simultaneously maintaining proper accuracy. Simplification is based on assumptions such as rectangular stress distribution in concrete, with a compressed zone depth  $\lambda x$  and a value of  $\eta f_{cd}$  ( $\lambda = 0.8$ ;  $\eta = 1.0$  – values for concrete grades from C12/15 up to C50/60) or a horizontal line at level  $f_{yd}$  on stress-strain graph for reinforcing steel. Due to such assumptions, stresses in steel are taken as proportional to strains, which can be presented in the following way:

- $\sigma_{si} = \varepsilon_{si} \cdot E_s$  if  $|\varepsilon_{si}| \leq \varepsilon_{yd}$
- $\sigma_{si} = f_{yd}$  if  $\varepsilon_{yd} < |\varepsilon_{si}| \leq 10\text{‰}$

In the current version of EC2 [17], there is no limitation of tensile reinforcement strains to 10‰ assuming a horizontal top branch of  $\sigma_s - \varepsilon_s$  diagram. Such a restriction can be applied, however, in the design procedures. Justification of such limitation can be found in [9] for example.

To draw an interaction curve, a system of two equations of forces equilibrium in the cross-section is used (equations for rectangular cross-sections are presented below):

- sum of longitudinal forces:

$$N_{Rd} = 0.8 \cdot f_{cd} \cdot b \cdot x + \sum_1^n \sigma_{si} \cdot A_{si} \quad (1)$$

- sum of moments on the axis parallel to the neutral axis, crossing the centre of concrete cross-section:

$$M_{Rd} = 0.8 \cdot f_{cd} \cdot b \cdot x \cdot (0.5 \cdot h - 0.4 \cdot x) + \sum_1^n \sigma_{si} \cdot A_{si} \cdot (0.5 \cdot h - a_i) \quad (2)$$

### 2.1. Method presented by R. Kliszczewicz [5]

According to this method (marked in the following part of an article as RK) five ranges of possible column's strains should be taken into consideration. The parameters of equations for the  $M_{Rd} - N_{Rd}$  interaction curves are:

- $\varepsilon_{c1}$  in the I range,
- $x$  in ranges II–IV,
- $\varepsilon_{s2}$  in the V range.

These ranges are given in Table 1 and presented in Fig. 3 and 4. Turns of forces in Fig. 4 were assumed in accordance to turns of acting forces. Attention should be paid to three issues. Firstly, the RK method allows to consider the reinforcement in the varied location of the section's height. Secondly, the effective depth of a cross-section  $d$  is treated here as a distance between the most compressed concrete fibre and the axis of the most distant reinforcement. Finally, values  $a_i$  are given as distances from the most compressed concrete fibre, as well.

Table 1

**Design ranges of partly-simplified method, according to [3]**

Range	$x$	Parameters of equilibrium equations	Reinforcing steel strains
I	$x = \frac{h}{0.8}$	$\frac{14}{23}‰ \leq \varepsilon_{c1} \leq 2‰$	$\frac{(0.002 - \varepsilon_{c1}) \cdot (3h - 7a_i)}{4h} \neq 0.002$
II	$h \leq x \leq \frac{h}{0.8}$	$x$	$0.002 \frac{7x - 7a_i}{7x - 3h}$
III	$\frac{7d}{27} \leq x \leq h$	$x$	$0.0035 \frac{x - a_i}{x}$

Table 1 – continued

IV	$0 \leq x \leq \frac{7d}{27}$	$x$	$-0.010 \frac{x - a_i}{x - d}$
V	$x = 0$	$-10\% \leq \varepsilon_{s2} \leq -10\% \frac{a_2}{d}$	$\varepsilon_{s2} - (0.010 + \varepsilon_{s2}) \frac{a_i - a_2}{d - a_2}$

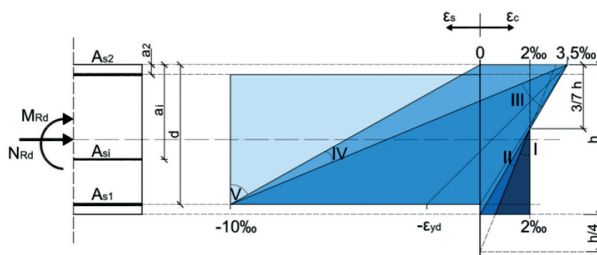


Fig. 3. Design ranges of partly-simplified method, according to [5]

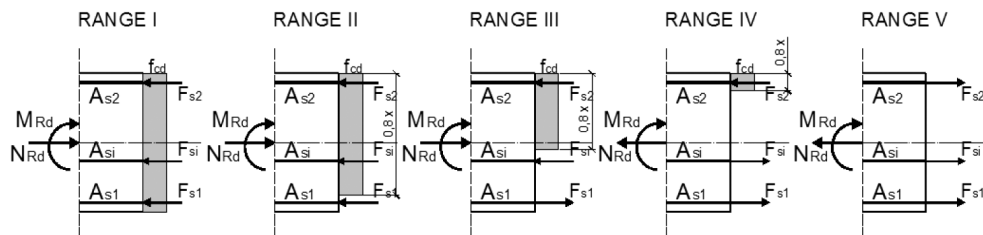


Fig. 4. Schemes for calculating load-bearing capacity for each range in RK method [5]

In ranges from I to IV, stress-strain distribution in compressed concrete zone is rectangular. In V range there is no compressed zone at all.

In all ranges,  $M_{Rd}$  and  $N_{Rd}$  values are calculated from equations (1) and (2); in the fifth range, an influence of concrete is omitted due to lack of compressed zone.

Ranges I and II apply to compression with very small eccentricity, when the neutral axis is placed beyond the cross-section. Stresses in concrete are equal to  $f_{cd}$ . Reinforcement in ranges I and II is compressed on the whole depth and stresses in steel can access value of  $f_{yd}$ .

$$\text{Range I: } x = \frac{h}{0.8} \text{ i } \frac{14}{23} \text{‰} \leq \varepsilon_{c1} \leq 2 \text{‰}$$

In range I, the whole cross-section is compressed. We assume that strains in reinforcement are proportional to  $\varepsilon_{c1}$  strains of the less compressed edge of concrete and that they are equal to:

$$\varepsilon_{si} = \frac{(0.002 - \varepsilon_{c1}) \cdot (3h - 7a_i)}{4h} + 0.002.$$

$$\text{Range II: } h \leq x \leq \frac{h}{0.8}$$

Stress distribution in the compressed zone (of depth  $0.8x$ ) does not cover the whole cross-section. An assumption is made that strains for each reinforcing bar are proportional to strains  $\varepsilon_c = 2\text{‰}$  of concrete in the distance of from the more compressed edge of concrete cross-section and are equal to:  $\varepsilon_{si} = 0.002 \frac{7x - 7a_i}{7x - 3h}$ .

$$\text{Range III: } \frac{7d}{27} \leq x \leq h$$

Stress distribution in the compressed concrete zone of depth equal to  $0.8x$  does not cover the whole cross-section; there are three possibilities of neutral axis location:

- neutral axis located between  $d$  and  $\frac{3}{7}h$  ( $d \leq x < h$ ) – reinforcement in the cross-section is not subjected to tension (the tension zone reaches no further than to the bottom reinforcement axis);
- compression zone depth is lower than effective depth of the cross-section  $\left( \frac{700d}{700 + f_{yd}} \leq x \leq d \right)$  – bottom reinforcement is subjected to tension, but its strains are lower than  $\varepsilon_{yd}$  and stresses do not reach the value of  $f_{yd}$
- neutral axis located from  $\frac{7d}{27} \leq x < \frac{700d}{700 + f_{yd}}$ ; reinforcement in the tensile zone can reach limit value of  $\varepsilon_s = -10\text{‰}$ ;

In whole range III, for each of neutral axis locations, we assume  $\varepsilon_{si} = 0.0035 \frac{x - a_i}{x}$ .

$$\text{Range IV: } 0 \leq x \leq \frac{7d}{27}$$

$A_{s1}$  reinforcement reaches limit strains  $\varepsilon_s = -10\text{‰}$ , while strains of the most compressed concrete fibre range from 0 to  $3.5\text{‰}$ ;

Strains in steel  $\varepsilon_{si}$  are calculated as proportional to limit values:  $\varepsilon_{si} = -0.010 \frac{x - a_i}{x - d}$ .

$$\text{Range V: } x = 0 \quad \text{and} \quad -10\text{‰} \leq \varepsilon_{s2} \leq -10\text{‰} \frac{a_2}{d}$$

This range applies to tension with a small eccentricity, when there is no compression zone in concrete. Strains in steel are then calculated according to the equation:

$$\varepsilon_{si} = \varepsilon_{s2} - (0.010 + \varepsilon_{s2}) \frac{a_i - a_2}{d - a_2}.$$

R. Kliszczewicz [5] presents two ways of evaluating interaction curves using these ranges and equations mentioned above.

First method:

In the aim of creating the right branch of the graph, an optimal number of parameters from described ranges is assumed, then stresses and strains in the reinforcement are calculated.

It allows for the determining of pairs of  $N_{Rd}$  and  $M_{Rd}$  using equations (1) and (2). The left side of the graph is obtained in case of symmetrical cross-section by reflecting the right branch of the graph towards the vertical axis of a coordinate system. In the case of non-symmetrical reinforcement, a theoretical 180 degrees rotation of the cross-section should be made and calculations have to be repeated.

Second method:

The right branch of the interaction curve is built by calculating the maximal and minimal values of longitudinal force  $N_{Rd}$ , for I range assuming  $\varepsilon_{c1} = 2\%$ , for  $V \varepsilon_{s2} = -10\%$  and dividing the obtained range into parts (depending on necessary accuracy). In this way, a set of coordinates of the graph is created.

Furthermore,  $N_{Rd}$  values are calculated for extremes of ranges and for designated  $N_{Rd}$  calculation of respective  $M_{Rd}$  values is made using iteration. This is how pairs of  $(M_{Rd}, N_{Rd})$  forces creating the right branch of the graph can be obtained. The left part is created as in the first method.

According to the authors of this article, while setting parameter values for which  $M_{Rd} - N_{Rd}$  pairs are calculated (especially when the division of range  $N_{Rdmax} - N_{Rdmin}$  is not very dense), a special point should not be omitted – the point relating to maximal moment ( $x = \xi_{eff,lim} \cdot d$ ,  $\varepsilon_{s1} = f_{yd} / E_s$ ).

## 2.2. Method presented by J. Procházka, A. Kohoutkova, J. Vaškova [16]

In the paper of J. Procházka, A. Kohoutkova, J. Vaškova [16], which is an academic book, a simpler method of creating interaction curves is presented. For the purposes of simplification, in the following part of this article, this method is described as PKV, from surnames of authors of the book [16]. Several specific strains are taken into consideration instead of ranges of strains – therefore, it is enough to calculate only 10 pairs of  $M_{Rd} - N_{Rd}$  values. Accuracy of this method is satisfactory in accordance with its simplicity and quickness. In the PKV method, a rectangular cross-section of stresses in concrete is assumed, with the compression zone depth equal to  $0.8x$ , constant value of stresses equal to  $f_{cd}$ , and a horizontal top branch of stress-strain distribution on reinforcing steel equal to  $f_{yd}$ . The PKV method only takes into account the reinforcement arranged at the top and bottom edge of the cross section. An example of the interaction curve obtained with the PKV method is shown in Fig. 5.

In Fig. 5, point A represents the load-bearing capacity of a cross-section subjected to axial compression with strains equal to 2%. It is respective to extreme value of the first range in RK method. This way the maximal  $N_{Rd}$  capacity for compression is designated.

Point B corresponds to a situation in which the depth of compression zone  $x$  is equal to an effective depth of the cross-section,  $d$ , which implicates zero strains in steel reinforcement  $A_{s1}$ . Strains in reinforcement  $A_{s2}$  are assumed as 3,5%. This case responds to the third range from the RK method.

Point C represents capacity of a cross-section in which the depth of the compression zone is equal to  $x_{lim} = \xi_{lim} \cdot d$ , which for the rectangular stress distribution in compressed concrete gives  $x_{eff,lim} = \xi_{eff,lim} \cdot d$ . Checks should be made as to whether  $x_{bal,1} = \xi_{bal,1} \cdot d \geq x_{bal,2} = \xi_{bal,2} \cdot a_2$ ,

where  $\xi_{bal,1}$  is equivalent for  $\xi_{lim} = \frac{\varepsilon_{cu,3}}{\varepsilon_{cu,3} + \varepsilon_{yd}}$ , and  $\xi_{bal,1} = \frac{\varepsilon_{cu,3}}{\varepsilon_{cu,3} - \varepsilon_{yd}}$ . If so, it can be assumed that both  $A_{s1}$  and  $A_{s2}$  reinforcement is completely used, which means that  $\sigma_{s1} = \sigma_{s2} = f_{yd}$ . With

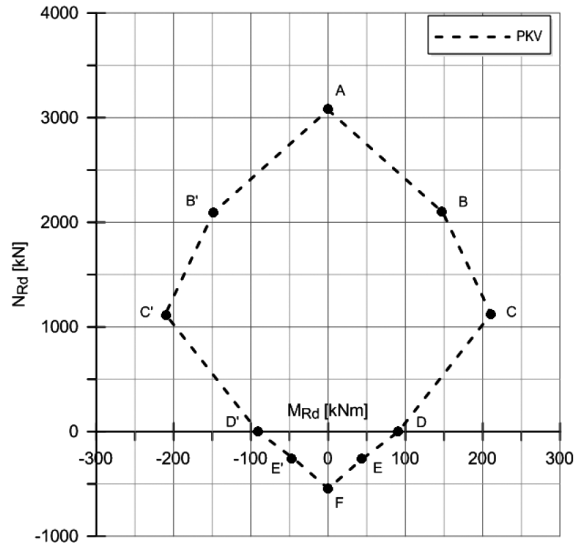


Fig. 5. An example of interaction curve according to PKV method [16]

such assumption, a maximum value of  $M_{Rd}$  is obtained. This case responds to the third range from the RK method.

Point D shows the capacity of a bended cross-section without axial force, it is a case which belongs to the fourth range. In the PKV method, an influence of compressed  $A_{s2}$  reinforcement is omitted.

Point E represents the capacity of a cross-section subjected to eccentric tension with a small eccentricity, the compression zone is omitted.

Point F shows the capacity of a cross-section subjected to axial tension. The bending moment is equal to zero. Reinforcements  $A_{s1}$  and  $A_{s2}$  are completely exploited. It is an example corresponding to an extreme value of a fifth range, from which we obtain maximal value of  $N_{Rd}$  for tension.

Points B', C', D', E' in case of symmetrical reinforcement can be designated by reflection towards the vertical axis. In cases when the reinforcement is not symmetrical, the cross-section should be theoretically rotated by 180 degrees and these points should be calculated with similar assumptions, treating reinforcement  $A_{s2}$  as  $A_{s1}$  and so on.

### 3. The comparison of $M_{Rd} - N_{Rd}$ interaction curves (according to RK and PKV methods)

The following part of the article consists of a comparison of interaction curves obtained from two described methods, RK and PKV, with assumptions:

- rectangular column cross-section with dimensions  $30 \times 40$  cm,
- C30/37 concrete grade
- RB500W steel,

- 3.0 cm cover,
- main reinforcement diameter:  $\phi$  20 mm,
- stirrups diameter:  $\phi_s$  6 mm,
- reinforcement ratio: 1.0% i 3.1%,
- symmetrical reinforcement, placed only at the top and bottom edge of the section.

Comparing these graphs (Fig. 6), it can be noted that the differences in results obtained from PKV methods in relation to those from the RK method are on the safe side. The advantages of the PKV method are its simplicity and the ability to perform calculations efficiently, such as in a spreadsheet.

If input data change and the reinforcement ratio is higher, e.g.  $\rho = 3.1\%$  ( $A_{s1} = A_{s2} = 18,85 \text{ cm}^2$ ), then point D of the PKV curve will not cover the curve from the RK method (Fig. 7). It is due to the fact that in the PKV method, compressed reinforcement is omitted while designating point D. The differences between these two methods in point D (moment value for zero axial force) will increase with an increasing reinforcement ratio or steel grade and with decreasing concrete strength.

Calculations for the PKV method can be simplified by omitting point E, because the curve for tension is close to linear.

$M_{Rd} - N_{Rd}$  interaction curves presented in the above figures were verified with curves obtained from computer software [10].

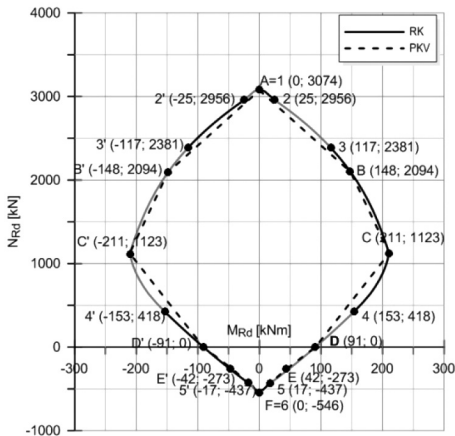


Fig. 6.  $M_{Rd} - N_{Rd}$  interaction curves according to RK [5] and PKV [16] methods, with  $\rho = 1.0\%$

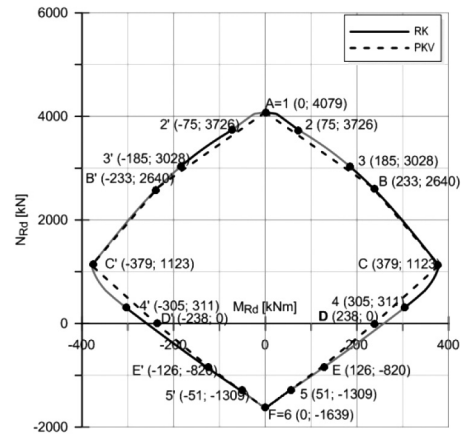


Fig. 7.  $M_{Rd} - N_{Rd}$  interaction curves according to RK [5] and PKV [16] methods, with  $\rho = 3.1\%$

#### 4. An example of using interaction curves to design thick reinforced concrete columns

To choose reinforcement for 47 columns of a vessel support structure interaction curves created with RK method were used. Dimensions of the cross-sections of the designed columns were equal to  $50 \times 50 \text{ cm}$  and could be analysed without considering second order effects. Columns were subjected to longitudinal forces and bending moments in both directions (skew

bending). The assumptions were made that there would be only four types of reinforcement (table 2) and that each type of reinforcement would be symmetrical and equivalent in both planes.

$M_{Rd} - N_{Rd}$  interaction curves were evaluated for these types of reinforcement. They take into account the whole reinforcement (not only concentrated on opposite sides, but also a part of it which is distributed parallel to the plane of bending).

Table 2

**Assumed types of vessel support structure reinforcement**

Column reinforcement	Reinforcement in both planes	Description in Fig. 8.
12 $\phi 16$	$A_{s1} = A_{s2} = 4\phi 16$	4 $\phi 16$
12 $\phi 25$	$A_{s1} = A_{s2} = 4\phi 25$	4 $\phi 25$
16 $\phi 25$	$A_{s1} = A_{s2} = 5\phi 25$	5 $\phi 25$
16 $\phi 28$	$A_{s1} = A_{s2} = 5\phi 28$	5 $\phi 28$

$M_{Rd} - N_{Rd}$  interaction curves for planes  $xy$ ;  $xz$ ; with points corresponding to pairs of  $M_{Ed} - N_{Ed}$  forces (representing the results of static calculations) are presented in Fig. 8. A preliminary increase of forces and moments by 50 percent has been made while putting  $M_{Ed} - N_{Ed}$  points onto interaction curves. Due to such an attitude, a designed reinforcement fulfils the EC2 [17] simplified criteria for skew bending:

$$\left(\frac{M_{Edz}}{M_{Rdz}}\right)^a + \left(\frac{M_{Edy}}{M_{Rdy}}\right)^a \leq 1.0 \tag{3}$$

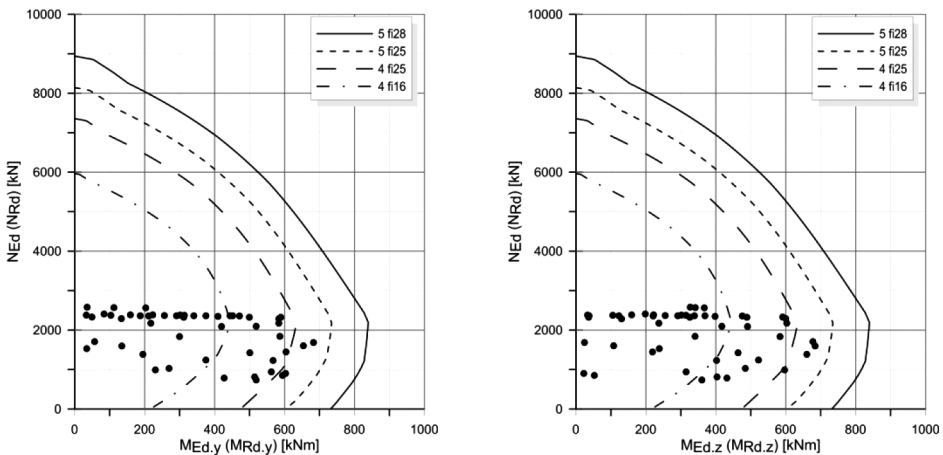


Fig. 8.  $M_{Rd} - N_{Rd}$  interaction curves in  $xy, xz$  planes. Preliminary choice of reinforcement for vessel support structure

The power  $\alpha$  has been assumed according to EC2 depending on the relation  $N_{Ed}/N_{Rd}$ .

After preliminary choice of reinforcement for skew bending according to interaction curves, the capacity of columns was checked. As a result, values fulfilling the normative conditions were obtained for all analysed columns.

It is important to include the reinforcement located along the section's height. A comparison of interaction curves which take into account only bars on opposite sides of the cross-section (dashed lines) with those taking into account all bars along the height of the section (solid lines) is shown in Fig. 9.

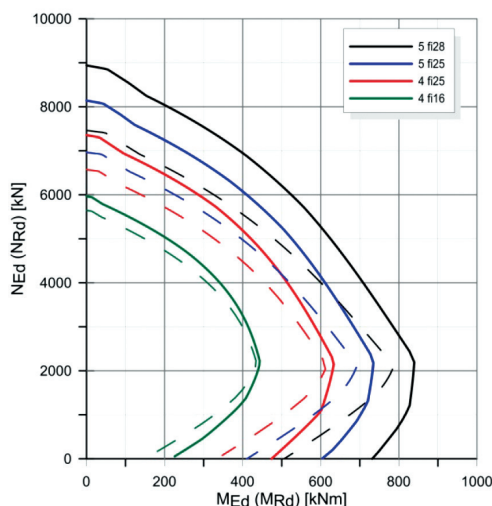


Fig. 9. The  $M_{Rd} - N_{Rd}$  interaction curves in  $xy$  and  $xz$  planes which take into account only the reinforcement located by the top and bottom edges (dashed line) and which take the whole reinforcement in the cross-section into account (solid line)

## 5. Second order effects on $M_{Rd} - N_{Rd}$ interaction curves

The following part of the article presents  $M_{Rd} - N_{Rd}$  interaction curves which take into consideration the reduction of capacity of columns due to second order effects. A comparison of an influence of chosen factors on the values of second order effects calculated with two simplified methods given by EC2 – nominal stiffness method (MNS) and nominal curvature method (MNC) was made.

### 5.1. Assumptions for analysis

Three cross-sections were analysed (as in Fig. 10), with the following data:

- rectangular column cross-section with dimensions  $40 \times 50$  cm,
- C30/37 concrete grade
- RB500W steel,
- $\gamma_c = 1.4$ ,

- $\gamma_s = 1.15$ ,
- 3.0 cm cover,
- main reinforcement diameter:  $\phi = 20$  mm,
- stirrups diameter:  $\phi_s = 6$  mm,
- symmetrical reinforcement as in Fig. 12.

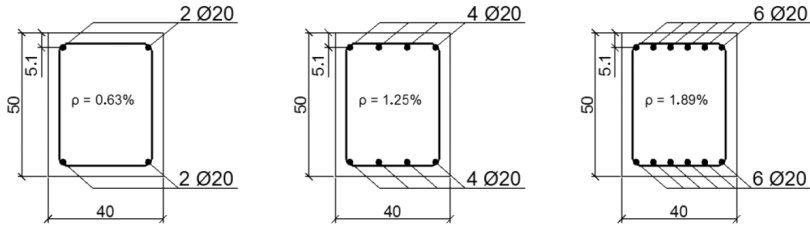


Fig. 10. Analysed cross-sections of columns

In the analysis, the following variable parameters were assumed, with values as follows:

- column slenderness:  $\lambda = 21; 35; 49$ ,
- $\lambda/\lambda_{lim}$  ratio = 0.5; 1.0; 2.0,
- reinforcement ratio  $\rho = 0.63\%; 1.25\%; 1.89\%$ ,
- effective creep coefficient  $\phi_{eff} = 0; 1.5$ .

In the MNS method, two assumptions were made – coefficient depending on first order moments distribution  $c_0 = 8$  (first order moment is constant,  $r_m = 1$ ), and coefficient depending on reinforcement ratio  $K_s = 1.0$ .  $K_c$  was calculated according to the formula 5.22 from EC2 [17]. In the MNC method, a distribution of total curvature was assumed to be sinusoidal, similarly for the second order effects. This approximation is on the safe side. For such curvature, a distribution of a coefficient  $c$  is equal to  $\pi^2 \approx 10$ . The  $n$  value for which the maximum limit value of a moment is achieved, was assumed as  $n_{bal} = 0.4$ .

## 5.2. Second order effects on $M_{Rd} - N_{Rd}$ interaction curves. Variable slenderness $\lambda$

Fig. 11a and b (below) present interaction curves with second order effects for columns with different slenderness. Second order effects were calculated with MNS and MNC for three different  $\lambda$  values, with assumed first order eccentricity  $e_0 = 0.07$  m (thus, for the values of moments  $m_1$  resultant from this eccentricity and from values of longitudinal forces).

The values of second order effects, obtained from the MNC method are presented in the whole range of loadings (similar to results considered in the engineer design of columns according to EC2), assuming stresses in steel equal to  $f_{yd}$ .

The following graphs (Fig. 11) present  $m_1$  values for first order impacts with imperfections and  $m_{II}$  values relevant for second order effects for  $n = 0.6$ . There is an increase of  $m_{II}$  with an increase of slenderness  $\lambda$ . For the analysed columns, values of second order effects from MNS and MNC differ significantly and this difference depends on the  $n$  level.

Fig. 12a and b present second order effects obtained from MNS and MNC for three different values of slenderness and corresponding imperfections measured from relevant lines. For the chosen value of  $n = 0.6$ , values of  $m_{imp}$  (moments from imperfections),

$m_{II}$  (second order moments),  $m_{static}$  (moments caused by loadings) were shown. Values of  $m_{II}$  were calculated not for assumed first order eccentricity as in the previous example, but for the highest possible values of  $m_{static}$  in relevance to capacity on a level of  $n$ .

The area between the interaction curve and a second order effects line for exact  $\lambda$  value is an area of possible values of  $m_{static}$ . By comparing the interaction curves for two methods, it can be concluded that this area is significantly smaller for MNS than from MNC.

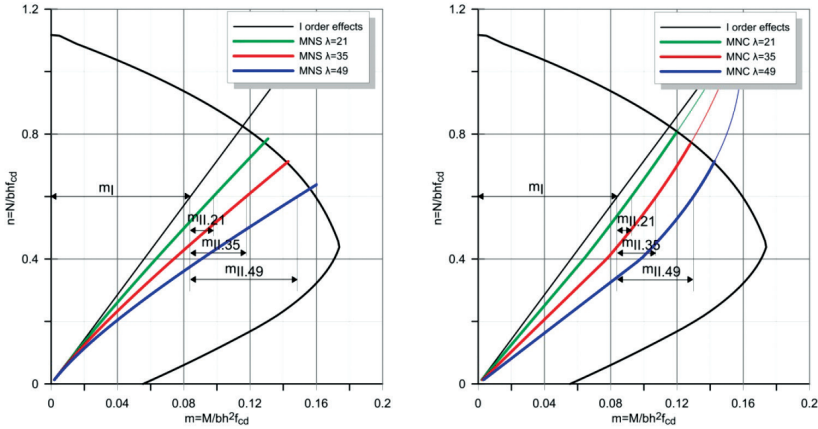


Fig. 11a, b.  $M_{Rd} - N_{Rd}$  interaction curves with second order effects for columns with different slenderness. Comparison of second order effects from MNS and MNC. Reinforcement ratio  $\rho = 0,63\%$ , effective creep coefficient  $\varphi_{eff} = 0$

Discontinuity of the graph obtained for  $\lambda = 49$  (Fig. 12a) with use of MNS, is caused by normative restriction of the value of  $k_2$  coefficient, which is used to consider the cracking and creep influence on the nominal stiffness of slender compressed concrete members.

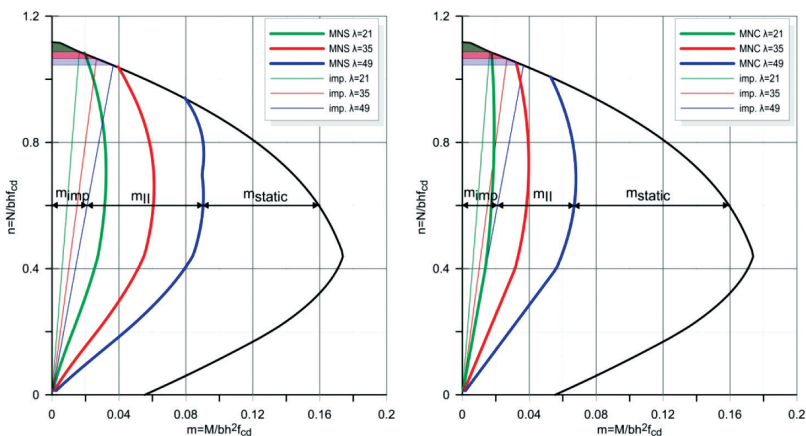


Fig. 12a, b.  $M_{Rd} - N_{Rd}$  interaction curves with second order effects (measured from imperfection line) for columns with different slenderness. Possible areas of  $m_{static}$  values calculated with MNS and MNC. Reinforcement ratio  $\rho = 0.63\%$ , effective creep coefficient  $\varphi_{eff} = 0$

To simplify using interaction curves with areas of possible values of  $m_{static}$ , second order effects can be measured from interaction curves as in Fig. 13a and b. The shadowed area represents possible first order moments for different forces  $n$  and slenderness  $\lambda$ ;  $m_I = m_{static} + m_{imp}$ .

Similar to former graphs,  $m_{II}$  moments were calculated for the biggest possible values of  $m_I$  due to capacity on the exact level of  $n$ .

Values of  $m_I$  and  $m_{II}$  designated for  $n = 0.6$  apply to slenderness  $\lambda = 49$ .

Comparing Fig. 13a and b, it can be noticed that an area of possible  $m_I$  values for the MNS method is significantly smaller than for MNC, this rule applies for each slenderness value.

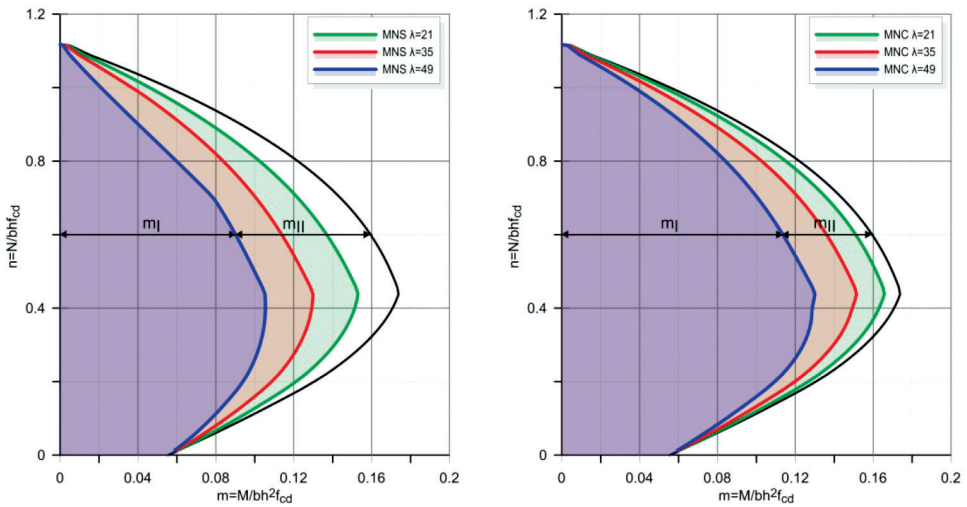


Fig. 13a, b.  $M_{Rd} - N_{Rd}$  interaction curves with second order effects (measured from interaction curves) for columns with different slenderness. Comparison of areas of possible  $m_I$  values according to MNS and MNC methods. Reinforcement ratio  $\rho = 0.63\%$ , effective creep coefficient  $\phi_{eff} = 0$

### 5.3. Second order effects on $M_{Rd} - N_{Rd}$ interaction curves – variable ratio of $\lambda/\lambda_{lim}$

$M_{Rd} - N_{Rd}$  interaction curves below (Fig. 14a, b) present second order effects calculated with MNS and MNC for a variable value of  $\lambda$  and for three different slenderness ratios  $\lambda/\lambda_{lim}$ , which equal 0.5; 1.0; 2.0, (with an assumed I order eccentricity  $e_0 = 0.07$  m). For chosen value of  $n = 0.6$  values of  $m_I$  and  $m_{II}$  were shown; for slenderness ratio  $\lambda/\lambda_{lim} = 2$ .

We can distinguish slight impact of slenderness lower than  $\lambda_{lim}$  and a significant influence of slenderness exceeding the limit value  $\lambda_{lim}$  on second order effects  $m_{II}$ .

For bigger values of  $\lambda/\lambda_{lim}$ , differences between second order effects calculated with MNS and MNC are more distinct.

Furthermore, for values of  $n < n_{bal}$  second order effects from MNS are lower than from MNC, whereas for  $n > n_{bal}$  the situation is opposite

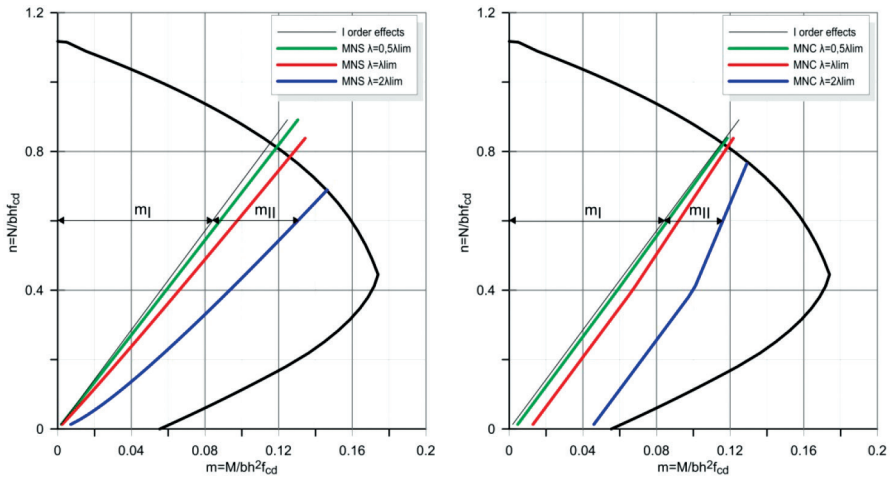


Fig. 14a, b.  $M_{Rd} - N_{Rd}$  interaction curves with second order effects calculated with MNS and MNC for columns with different slenderness  $\lambda/\lambda_{lim}$  ratios. Reinforcement ratio  $\rho = 0.63\%$ , effective creep coefficient  $\phi_{eff} = 0$

5.4. Second order effects on  $M_{Rd} - N_{Rd}$  interaction curves – variable reinforcement ratio  $\rho$

The following  $M_{Rd} - N_{Rd}$  interaction curves (Fig. 15a, b) present second order effects calculated with MNS and MNC for three different reinforcement ratios  $\rho = 0.63; 1.25; 1.89$  (with an assumed first order eccentricity equal to  $e_0 = 0.07$  m).

For the chosen value of  $n = 0.8$ , values of  $m_I$  and  $m_{II}$  relevant for reinforcement ratio  $\rho = 1.89\%$  were presented.

In graphs considering MNS an influence of reinforcement ratio on second order effects  $m_{II}$  is clear; however graph for MNC claims that values of second order effects  $m_{II}$  are not dependent on reinforcement ratio.

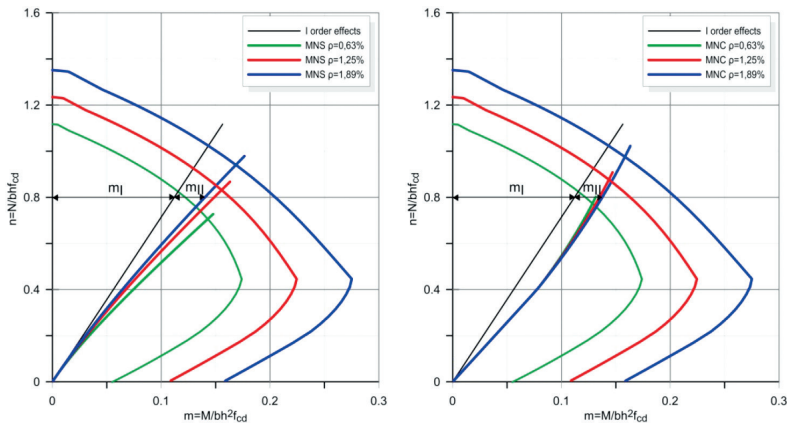


Fig. 15a, b.  $M_{Rd} - N_{Rd}$  interaction curves with second order effects calculated with MNS and MNC for various reinforcement ratio. Column slenderness  $\lambda = 35$ , effective creep coefficient  $\phi_{eff} = 0$

### 5.5. Second order effects on $M_{Rd} - N_{Rd}$ interaction curves – variable creep coefficient

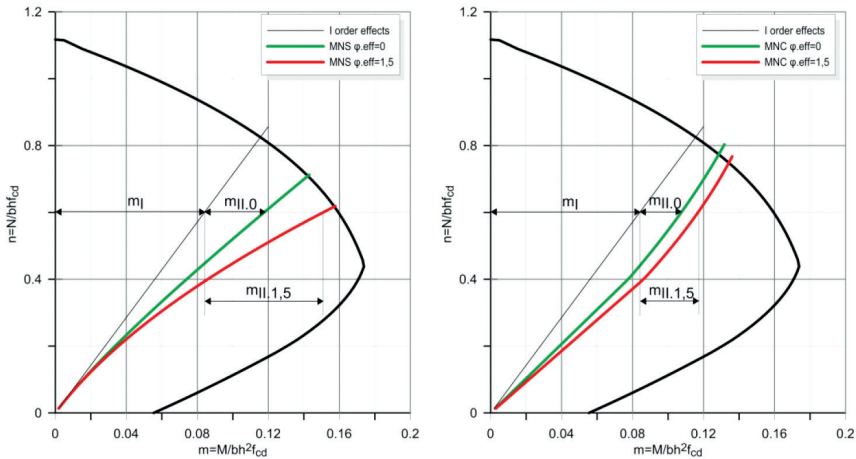


Fig. 16a, b.  $M_{Rd} - N_{Rd}$  interaction curves with second order effects calculated with MNS and MNC for various creep coefficient  $\varphi_{eff}$ . Column slenderness  $\lambda = 35$ , reinforcement ratio  $\rho = 0.63\%$

Fig. 16a and b, present second order effects calculated with MNS and MNC on  $M_{Rd} - N_{Rd}$  interaction curves for creep coefficients equal to  $\varphi_{eff} = 0$  and  $\varphi_{eff} = 1.5$  (with an assumed first order eccentricity equal to  $e_0 = 0.07$  m). For the chosen value of  $n = 0.6$ , values of  $m_I$  and  $m_{II}$  relevant for creep coefficient  $\varphi_{eff} = 0$  were presented. In analysed cases for  $n > n_{bal}$  the impact of creep on second order effects  $m_{II}$  calculated with MNS is higher than on second order effects from MNC.

## 6. Conclusions

The first part of the paper presents two methods of evaluating  $M_{Rd} - N_{Rd}$  interaction curves for members subjected to axial force and bending moment in one plane (partly-simplified RK and PKV methods) [5, 16]. It was proven that despite the different assumptions in methods PKV and RK, results obtained from both methods are similar. There was also an example of applying the interaction curves to the choice of the reinforcement in vessel support structure.

The second part of the paper considers the reduction in  $M_{Rd} - N_{Rd}$  interaction curves due to second order effects. Interaction curves were designated with RK method. Second order effects were calculated with methods of nominal stiffness and nominal curvature, according to EC2, for various values of slenderness,  $\lambda/\lambda_{lim}$  ratio, reinforcement ratio  $\rho$  and creep coefficient  $\varphi_{eff}$ .

The usefulness of  $M_{Rd} - N_{Rd}$  interaction curves not only for designing and checking the capacity of columns, but also for analysis, such as the one carried out in this article – comparing second order effects evaluated with different methods, was indicated in the article.

On the basis of the conducted analysis:

- it was proved that second order effects calculated with MNS and MNC differ significantly, their comparison was presented on  $M_{Rd} - N_{Rd}$  interaction curves
- it was claimed that differences between second order effects from MNS and MNC depend on the value of  $n = N_{Ed}/bhf_{cd}$ ,
- it was noticed that for the analysed column, the area of possible  $m_{static}$  values for second order effects from MNS is considerably lower than from MNC
- an increase of  $m_{II}$  value with an increase of ratio of slenderness to its limit value  $\lambda/\lambda_{lim}$  in MNS and MNC and its dependence on  $n/n_{bal}$  ratio was presented
- the differences between an impact of reinforcement ratio on second order effects were shown; this influence is distinct in MNS and inconsiderable in MNC *confusing sentence – we usually expect to see differences between something and something else.*
- it was presented that the influence of creep on second order effects in MNC is lower than in MNS.

The comparisons of second order effects calculated by MNS and MNC methods presented in the paper, are aimed at depicting the situation encountered by the designer applying the rules of Eurocode 2 [17] and to indicate the need for comments to this standard (standard czy code? Tu sama nie jestem pewna, raczej code – od Eurocode chociażby), which could help to choose the right method.

## References

- [1] *Podstawy projektowania konstrukcji betonowych i żelbetowych według Eurokodu 2*, praca zbiorowa pod redakcją M. Knauffa, Dolnośląskie Wydawnictwo Edukacyjne, Wrocław 2006.
- [2] *CEB/FIP Manual on Bending and Compression Design of Sections under Axial Action Effects at the Ultimate Limit State*, Bulletin d'Information, No. 141, 1982.
- [3] *Model Code 2010. Final draft*, April 2012.
- [4] Knauff M., *Obliczanie konstrukcji żelbetowych wg Eurokodu 2. Zasady ogólne i zasady dotyczące budynków*, Wydawnictwo Naukowe PWN, Warszawa 2012.
- [5] Kliszczewicz R., *Konstrukcje betonowe. Obliczanie elementów żelbetowych w stanach granicznych nośności i użytkowania wg PN-B-03264:2002*, Wydawnictwo Politechniki Śląskiej, Gliwice 2008.
- [6] Bažant Z.P., Cedolin L., Tabbara M.R., *New method of analysis for slender columns*, ACI Structural Journal; July–August 1991, 391-401.
- [7] Kamińska M.E., *High-strength concrete and steel interaction in RC members*, Cement & Concrete Composites 24, 2002, 281-295.
- [8] Westerberg B., *Second order effects in slender concrete structures. Background to the rules in EC2*, Betongbyggnad, 2004.
- [9] Czkwianianc A., Kamińska M., *Nośność przekrojów obciążonych momentem zginającym i siłą podłużną*, w: *Podstawy projektowania konstrukcji betonowych i żelbetowych według Eurokodu 2*, praca zbiorowa pod redakcją M. Knauffa, Dolnośląskie Wydawnictwo Edukacyjne, Wrocław 2006.
- [10] Program KBB udostępniony przez Politechnikę Łódzką.

- [11] Pallarés L., Bonet J.L., Fernandez M.A., Miguel P.F., *C<sub>m</sub> factor for non-uniform moment diagram in RC columns*; Engineering Structures 31, 2009, 1589-1599.
- [12] Cortés-Moreno E., Bonet J.L., Romero M.I., Miguel P.F., *Slenderness limit of the weak axis in the design of rectangular reinforced concrete non-sway columns*, Engineering Structures 33, 2011, 1157-1165.
- [13] Csuka B., Kollár L., *Design of reinforced concrete columns under centric load according to Eurocode 2*, Concrete Structures, 2011.
- [14] Feix J., Walkner R., *Betonbau. Grundlagen der Bemessung nach EC2*, Studia Universitätsverlag, 2012.
- [15] Fingerloos F., Hegger J., Zilch K., *Eurocode 2 für Deutschland: DIN EN 1992-1-1 Bemessung und Konstruktion von Stahlbeton- und Spannbetontragwerken. Teil 1-1, Kommentierte Fassung*; Berlin, Wien, Zürich, 2012.
- [16] Procházka J., Kohoutkova A., Vaškova J.: *Příklady navrhování betonových konstrukcí 1*, ČVUT, Praga 2007.
- [17] PN-EN 1992-1-1:2008 – Eurokod 2. Projektowanie konstrukcji z betonu. Część 1-1: Reguły ogólne i reguły dla budynków.
- [18] Lechman M., *Wymiarowanie przekrojów elementów z betonu zginanych z udziałem siły osiowej według Eurokodu 2. Przykłady obliczeń*, Instytut Techniki Budowlanej, Warszawa 2011.